International Journal of Pharmaceutics 358 (2008) 256–262

Contents lists available at ScienceDirect

International Journal of Pharmaceutics

journal homepage: www.elsevier.com/locate/ijpharm

Pharmaceutical Nanotechnology

Simultaneous synthesis and coating of salbutamol sulphate nanoparticles with L-leucine in the gas phase

Anna Lähde [a], Janne Raula [a], Esko I. Kauppinen [a,b,*]

[a] NanoMaterials Group, Laboratory of Physics & Center for New Materials, Helsinki University of Technology, P.O. Box 5100, FI-02015 TKK, Finland
[b] VTT Biotechnology, P.O. Box 1000, FIN-02044 VTT, Finland

ARTICLE INFO

Article history:
Received 19 December 2007
Received in revised form 4 February 2008
Accepted 9 February 2008
Available online 7 March 2008

Keywords:
Aerosol
Coating
L-Leucine
Nanoparticles
Pharmaceutical
Physical vapor deposition
Salbutamol sulphate

ABSTRACT

Salbutamol sulphate nanoparticles have been simultaneously prepared and coated with L-leucine in the gas phase. Three different ways of coating can be separated based on the operation temperatures used in an aerosol flow reactor. Below the temperature of L-leucine sublimation, formation of the L-leucine layer on the core particle surface takes place via diffusion of L-leucine molecules on the droplet surfaces during droplet drying. At intermediate temperatures, the extent of sublimation of L-leucine depends notably on the concentration, and thus partial evaporation was expected. The L-leucine coating was solely formed via vapor deposition at high reactor temperatures when complete sublimation of L-leucine was obtained. The geometric mean diameter of the core salbutamol particles was approximately 65 nm. In general, particle size increased with the addition of L-leucine. The size distribution remained the same or broadened when the coating layer of the particles was formed via surface diffusion whereas notable narrowing of the distribution was observed when the coating was formed via vapor deposition. Upon desublimation and heterogeneous nucleation on the surfaces of smooth, spherical core particles, L-leucine formed a discontinuous coating with leafy crystals a few nanometers in size.

1. Introduction

Various applications of pharmaceutical nanoparticles have been proposed, such as tissue targeting in cancer therapy (Brigger et al., 2002), controlled release (Peltonen et al., 2002) and improvement in the solubility of poorly soluble drugs (Chen et al., 2002). Due to the large surface area per unit mass of nanoparticles, they show increased surface activity as well as biological reactivity, e.g., antioxidant activity and penetration of cellular barriers (Obersdörster et al., 2005). The ratio of surface atoms that determine the properties of the material increases exponentially with decreasing particle size (Obersdörster et al., 2005). However, the production of nanoparticles, that are stable and do not fuse together, i.e., form large aggregates, is a challenge. Such structural stabilization of particles has been carried out by coating them with stabilizing agents (Yang et al., 2005). Moreover, this surface modification enables the optimization of material behavior in various dosage forms and in controlled delivery systems and provides increased efficacy and reduced toxicity of a drug at the site of action (Ravi Kumar, 2000).

Reduced surface forces result in improved powder flowability and dispersibility. For the manipulation of the forces a good example for surface modification is the use of surface-active amino acids, particularly L-leucine analogues that enrich on the core particle surfaces (Chew et al., 2005; Lechuga-Ballesteros and Kuo, 2001; Lucas et al., 1999). Among surface modifying materials L-leucine has been shown to improve powder properties and to stabilize micron-sized particles at moderate humidities (Raula et al., 2008). However, L-leucine has not been previously considered as a stabilizing agent for nano-sized particles that are known to agglomerate and sinter very easily. Apart from used material, a proper tailoring of coating is also of utmost importance for particle stability.

Several different techniques have been studied for the production of surface modified and coated pharmaceutical particles. These methods can be broadly divided into dry and wet techniques. The dry methods rely on strong mechanical forces which bring the small quest particles of approximately 0.02–2 μm in size into contact with relatively large host particles of more than 10 μm in size (Yang et al., 2005). This is done using, for example, conventional powder mixers (Pfeffer et al., 2001) or with a more advanced magnetically assisted impaction coating method (Ramlakhan et al., 2000). These techniques are used to improve properties such as dispersibility and flowability of the powder (Yang et al., 2005). The wet techniques include emulsions and suspensions where particles are formed and stabilized in a solution

* Corresponding author at: NanoMaterials Group, Laboratory of Physics & Center for New Materials, Helsinki University of Technology, P.O. Box 5100, FI-02015 TKK, Finland. Tel.: +358 40 509 8064.
E-mail address: esko.kauppinen@hut.fi (E.I. Kauppinen).

0378-5173/$ – see front matter © 2008 Elsevier B.V. All rights reserved.
doi:10.1016/j.ijpharm.2008.02.027

(Cooney and Hickey, 2003; Murakami et al., 1999). However, the particles in solution should be lyophilized in order to improve the stability of the particles (Bodmeier et al., 1991; Schmidt and Bodmeier, 1999). An emulsion solvent evaporation technique has been used to dry drug nanoparticles in aqueous solutions (Edwards et al., 1997). In addition, a fluidized bed (Ichikawa and Fukumori, 1999) and spray drying (Ré, 1998) have been used which involves the particles being suspended in the gas phase. These techniques, however, cannot be used for the coating of nano-sized particles. Dry coated nano- and micron-sized particles can be produced using an evaporation–condensation technique, e.g., chemical and physical vapor deposition (Choy, 2003; Gurav et al., 1993; Mattox, 1998; Pillai et al., 1994; Zhang et al., 2004).

We describe the simultaneous synthesis and surface modification of nano-sized salbutamol sulphate particles in the gas phase using L-leucine vapor. This novel gas phase coating method was introduced for micron-sized particles by Raula et al. (2008). Depending on the partial vapor pressure of L-leucine in the reactor, different mechanisms for the formation of the L-leucine coating layer were observed. Below the temperature of L-leucine sublimation, the coating was formed by the diffusion of L-leucine molecules within droplets whereas above this temperature the coating was formed by physical vapor deposition of L-leucine on the core particle surfaces. The former coating method relies on the surface-active property of L-leucine (Weissbuch et al., 1990) which drives these molecules to air–water interfaces of aqueous droplets. Prior to the latter coating process, L-leucine sublimes (Budavari et al., 1989; Svec and Clyde, 1965) and, upon rapid cooling, this vapor nucleates on the surface of the core particles where the coating grows due to vapor deposition. This work explored the saturation conditions which control the sublimation of L-leucine and the formation of the coated salbutamol nanoparticles in the gas phase.

2. Materials and methods

2.1. Materials

The core material salbutamol sulphate (Alfa Aesar, Germany) and the coating material L-leucine (Fluka, Switzerland) were used as received. The concentrations in the precursor solutions were 4 g/l for salbutamol sulphate and 0, 0.5, 1.1, 2.2, 4.3, and 17.2 g/l for L-leucine in ion-exchanged water of pH 6 (Millipore). The resulting precursor solutions were clear to indicate a complete dissolution of L-leucine.

2.2. Nanoparticle production

Fig. 1 shows the experimental set-up of the aerosol reactor used in the experiments. The precursor solution was atomized with a constant output atomizer in the recirculation mode (TSI Instruments, model 3076), see Feeding in Fig. 1. A flow rate of 3.3 l/min of carrier gas (nitrogen, N_2) was used. The actual average feed rate of precursor solution to the reactor was 0.079 ml/min. This gave estimated L-leucine concentrations in the reactor assuming no losses (C_{re}) of 0.01, 0.03, 0.05, 0.10 and 0.41 g/m^3 (Table 1) corresponding to L-leucine concentrations (C_{le}) of 0.5, 1.1, 2.2, 4.3 and 17.2 g/l in the precursor solutions, respectively. The salbutamol concentration was constant (C_{sal}) at 0.10 g/m^3 corresponding to a precursor solution concentration of 4 g/l.

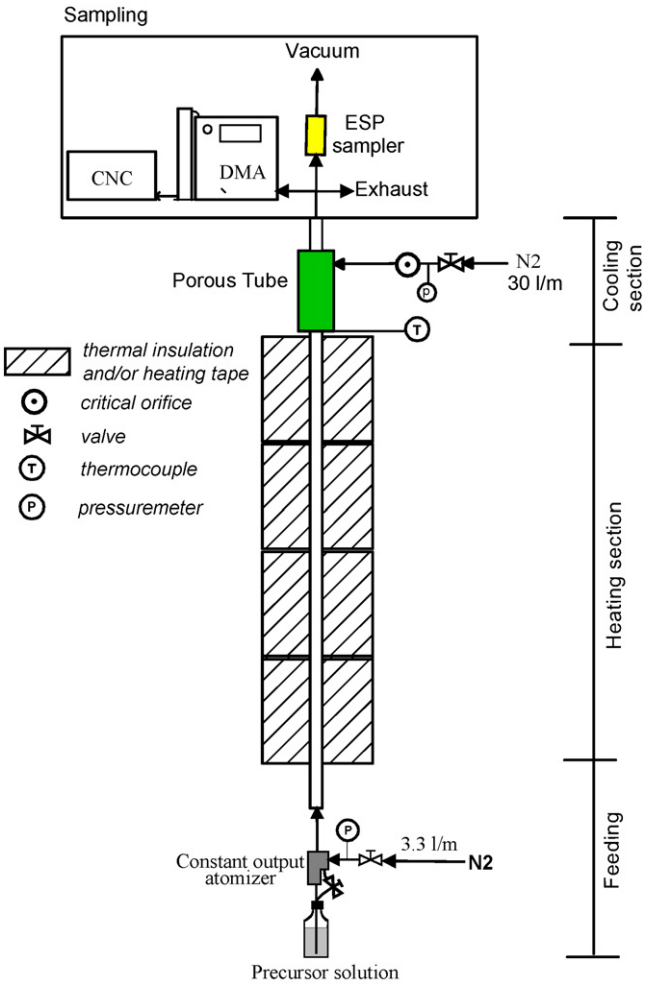

Fig. 1. The experimental set-up. Different reactor sections are presented: (1) feeding, (2) heating, (3) cooling and (4) sampling.

After atomization, the droplets were carried to the heated zone of the reactor, which consisted of a stainless steel tube (inner diameter of 30 mm and length of 1200 mm) placed inside the furnace (see Heated section in Fig. 1). The temperature in the heated zone

Table 1
A summary of experimental conditions for the production of salbutamol/L-leucine particles produced at heated zone temperature (T_H) between 110 and 200 °C

Concentration of L-leucine		S_{HEAT} (T_H = 110–200 °C)	T_{cal} [°C]	T_{onset} [°C]	v [°C/ms]	S_{COOL}
In solution, C_{le} [g/l]	In reactor, C_{re} [g/m^3]					
0.5	0.01	$1–3.9 \times 10^{-3}$	140	110–130	0.2–0.4	19
1.1	0.03	$1–7.8 \times 10^{-3}$	147	130–140	0.2–0.4	38
2.2	0.05	$1–1.6 \times 10^{-2}$	154	130–140	0.2–0.4	76
4.3	0.10	$1–3.1 \times 10^{-2}$	161	145–155	0.2–0.4	151
17.2	0.41	$1–1.2 \times 10^{-1}$	175	160–170	0.2–0.4	604

C_{le} and C_{re} are the L-leucine concentration in the precursor solution and the reactor, respectively, S_{HEAT} is the calculated saturation ratio corresponding to heated zone temperatures, T_{cal} is the sublimation temperature of L-leucine calculated based on the L-leucine vapour pressure, and T_{onset} is the temperature range where the sublimation was observed in the experiments. In the cooling section of the reactor v is the cooling rate and S_{COOL} is the momentary saturation ratio of L-leucine calculated at 96 °C that corresponds to the temperature at the exit of porous tube at T_H of 200 °C.

was varied from 110 to 200 °C. The flow in the heated zone was fully laminar with Reynolds number between 126 at 110 °C and 108 at 200 °C and the residence times were changed accordingly from 11.8 to 9.6 s. The centerline gas temperatures of the reactor tube were measured with gas flow on at 5 cm intervals with a K-type thermocouple. Target temperature was reached at 40 cm from the reactor inlet and was constant (±1 °C) until the exit of the heated zone. The temperature and flow profiles of the aerosol flow reactor have been simulated with computational fluid dynamics (CFD) calculations described elsewhere (Lähde et al., 2006). The residence time at the target temperature was sufficient for complete evaporation of L-leucine (Raula et al., 2007).

The aerosol exiting the heated zone was rapidly cooled with a large volume of N_2 at ambient temperature with a flow rate of 30 l/min, see Cooling section in Fig. 1. The cooling gas was introduced using a sintered metal porous tube with the length of 200 mm, an inner diameter of 12.7 mm and the pore size 20 μm. Fig. 2 shows the temperature profiles in the heated and cooling zones of the reactor at different temperatures. In this section, if the reactor temperature was high enough for L-leucine to sublime, the nucleation and subsequent deposition of L-leucine vapor were initiated. The cooling gas also diluted the aerosol with a volume ratio of 10:1 that prevented water condensation and decreased the deposition losses of particles on the reactor walls. Complete mixing of aerosol and cooling gas occurred in a mixing tube with an inner diameter of 9.6 mm and length of 250 mm before particle sampling. The flow Reynolds number in the porous tube and the mixing tube ($Re \sim 4550$) indicated turbulent flow. Table 1 summarizes the main experimental parameters including concentrations, sublimation temperatures and saturation conditions for the preparation of L-leucine coated salbutamol nanoparticles.

2.3. Instrumentation and characterization

The sampling of particles is shown in sampling in Fig. 1. The particle number size distributions were measured with a differential mobility analyzer, DMA (TSI Instruments, model 3081) connected to a condensation nucleus counter, CNC (TSI Instruments, model 3022). Particle samples were collected with a point-to-plate electrostatic precipitator, ESP (InTox Products) on carbon coated copper grids (Agar Scientific Ltd.). The structure of the particles was studied with a field emission low voltage scanning electron microscope, FE-SEM (Leo Gemini DSM982). For SEM imaging, the samples were sputter-coated with platinum to increase particle stability under the electron beam.

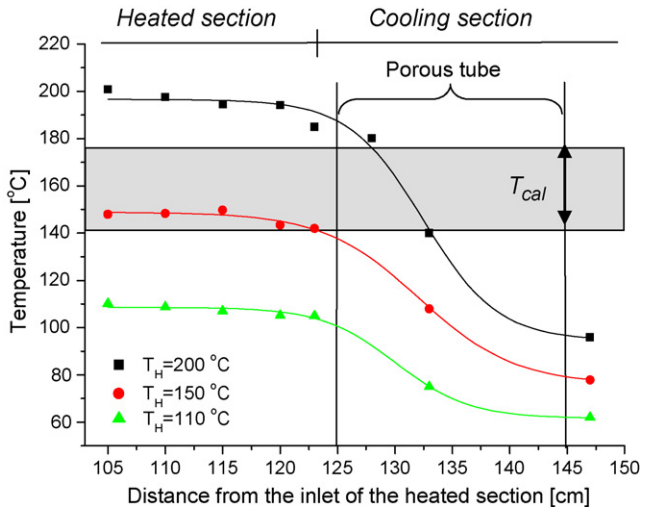

Fig. 2. The centerline temperature profiles of the reactor at the temperatures (T_H) of 110 °C, 150 °C and 200 °C in the heated section. The cooling gas temperature was 22 °C. The gray window shows the range of calculated temperatures (T_{cal}) where saturation ratio of L-leucine is fixed to unity for the L-leucine vapour concentration from 0.013 to 0.41 g/m^3. The placement of the porous tube in the cooling zone is shown in the figure.

2.4. Saturation ratio of L-leucine in the reactor

The vapor pressure and saturation ratio of L-leucine in the reactor was calculated using the enthalpy of sublimation (H_{sub} = 150.7 kJ/mol at T_{sub} = 455 K) according to Svec and Clyde (1965). Saturation vapor pressure (p_s) was calculated using the equation

$$p_s = p^* e^{-C} \quad \text{with} \quad C = \frac{\Delta H_{sub}}{R}\left(\frac{1}{T_H} - \frac{1}{T_{sub}}\right), \tag{1}$$

where p^* is the vapor pressure at the temperature of T_{sub}, T_H is the temperature in the heated zone, ΔH_{sub} is the enthalpy of sublimation, R is the gas constant. The partial vapor pressure (p) of L-leucine in the reactor was calculated using the equation

$$p = \frac{qRT_H}{MQ_R}, \tag{2}$$

where q is the mass of L-leucine fed to the reactor [g/min], M is the molecular weight of L-leucine, and Q_R is the temperature corrected flow rate of nitrogen gas. Instantaneous perfect mixing was assumed and the temperature gradient between the center line and the walls of the reactor was not taken into account. The saturation ratio was estimated according to the relation

$$S = \frac{p}{p_s}. \tag{3}$$

The vapor pressure and saturation ratio of water in the reactor were also calculated using Eqs. (1)–(3). The saturation vapor pressure of water at different temperatures was taken from the literature (Incropera and DeWitt, 2002). The saturation ratios of water were well below zero at all reactor conditions.

3. Results and discussion

3.1. Sublimation of L-leucine

It should be noted that the temperatures discussed here refer to the temperatures in the heated section of the reactor (T_H), where both the drying of droplets and the sublimation of L-leucine took place. The sublimation and particle formation of pure L-leucine in an aerosol flow reactor has been studied by Raula et al. (2007). The actual coating, i.e., nucleation and subsequent vapor deposition of L-leucine on the surface of salbutamol core particles occurred in the cooling section of the reactor (Fig. 1). Saturation conditions of L-leucine in the heated zone of the reactor were estimated using Eqs. (1)–(3). Accordingly, the sublimation of L-leucine was expected to initiate when the reactor temperature was raised above the temperatures (T_{cal}) that were calculated by setting the saturation ratio to unity (Fig. 2). These temperatures were 140, 147, 154, 161 and 175 °C for L-leucine concentrations of 0.01, 0.03, 0.05, 0.10 and 0.41 g/m^3 in the reactor (Table 1). The rapid cooling with large gas volume induced a sudden change in saturation conditions leading to the supersaturation of L-leucine vapor (S_{COOL} in Table 1).

Fig. 3 shows the number size distributions of the salbutamol/L-leucine particles produced at different reactor temperatures (T_H) with L-leucine concentration of 0.10 g/m^3. The number size distribution of salbutamol core particles remained constant in all conditions with the geometric number mean diameter 65 nm. In

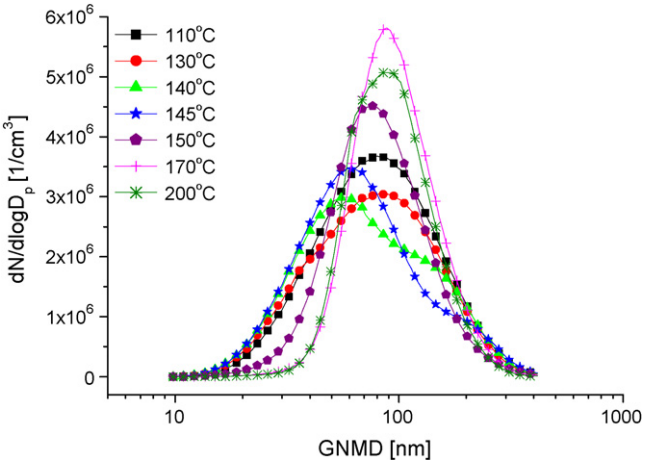

Fig. 3. Number size distribution ($dN/d\log D_p$) of the salbutamol/L-leucine particles prepared at different temperatures of the heated section. The salbutamol and L-leucine concentrations were $C_{sal} = 0.10\ g/m^3$ and $C_{re} = 0.10\ g/m^3$, respectively.

case of salbutamol/L-leucine particles, the original monomodal distribution changed at a certain temperature, first, to bimodal or to a distribution with a shoulder and then, upon a further increase in temperature, to narrowly distributed monomodal distribution. This, however, did not apply with the highest L-leucine concentration, which will be discussed later.

The precise determination of the onset temperatures for L-leucine sublimation in the reactor was difficult to perform. However, the temperature ranges where the sublimation of L-leucine took place can be estimated. The ranges were estimated between the two temperatures where size distributions changed, e.g., distribution narrowing or shoulder formation. The temperature ranges for sublimation were 110–130, 130–140, 130–140, 145–155, and 160–170 °C for L-leucine concentrations of 0.01, 0.03, 0.05, 0.10, and 0.41 g/m^3, respectively. Accordingly, sublimation of L-leucine occurred at lower temperatures than the estimated calculated sublimation temperatures (see above). This is understood by the Kelvin effect, which means that thermal transitions like melting and vaporization of material requires less energy when particle size decreases (Dick et al., 2002; Jiang et al., 1999, 2000; Lai et al., 1996; Zhao and Jiang, 2004). For particles composed of organic material the Kelvin effect can be significant for particle sizes up to 200 nm (Seinfeld and Pandis, 2006). Thus, the sublimation of L-leucine from nanoparticles occurred at lower temperatures than the sublimation temperatures calculated for bulky material.

3.2. Formation of L-leucine coated particles

The formation of L-leucine coating on the surface of salbutamol sulphate particles can be divided into three main cases according to the saturation conditions of L-leucine: Case I, no sublimation of L-leucine and thus particles were formed purely by droplet drying, i.e., evaporation of solvent water; Case II, L-leucine was partially sublimed. Upon cooling, L-leucine vapor deposits on the core particle surfaces via heterogeneous nucleation; Case III, L-leucine was completely sublimed at all concentrations and the vapor may undergo either heterogeneous nucleation on the surface of salbutamol core particles and/or homogeneous nucleation producing new L-leucine particles. Accordingly to the Cases I–III, Fig. 4 shows the number size distribution of the salbutamol/L-leucine particles prepared at T_H 110, 150 and 200 °C. In general, particle size increased during the course of L-leucine addition. The size distribution of particles with $C_{re} = 0.41\ g/m^3$ prepared at 110 °C had

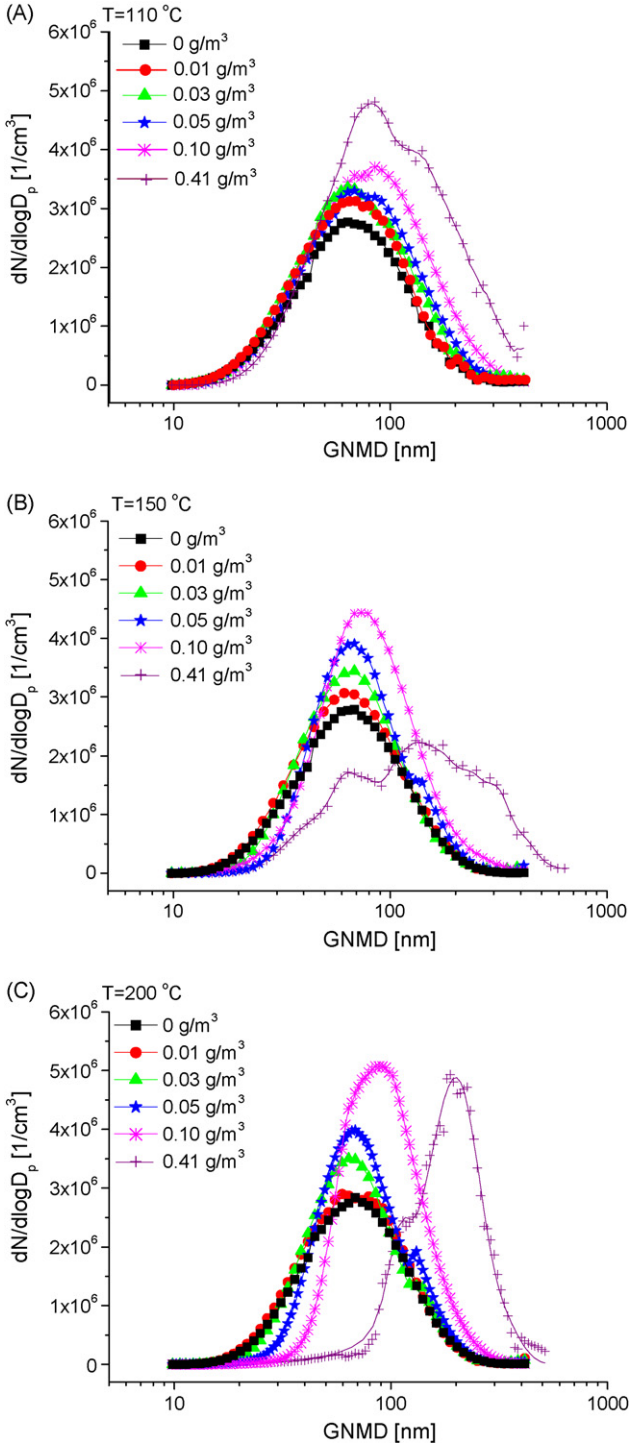

Fig. 4. Number size distributions of uncoated salbutamol and salbutamol/L-leucine particles prepared in the reactor where the temperatures in the heated section were (A) 110 °C, (B) 150 °C and (C) 200 °C. The salbutamol and L-leucine concentrations were $C_{sal} = 0.10\ g/m^3$ and $C_{re} = 0–0.41\ g/m^3$, respectively.

a shoulder at a size of 150 nm that was indicative of the formation of two kinds of particles (Fig. 4A). This distribution can be explained as follows: L-leucine is a surface-active material that accumulates on an air–water interface which, in this study, was the surface of droplets (Weissbuch et al., 1990). Once droplets were produced, L-leucine molecules enrich on droplet surfaces to form a film. The film prevented the free penetration of vaporized water molecules leading to a build-up of pressure inside the particles. The

pressure expanded the L-leucine film which finally broke the particles into smaller fractures observed as bimodal size distribution. Moreover, along with the temperature increase, the evaporation rate of water increased thus facilitating particle breakage upon drying (Fig. 4B). This obviously increased geometric standard deviation (G.S.D.) prior to L-leucine sublimation. In Case III at T_H of 200 °C, L-leucine vaporized completely in the heated section of the reactor in all concentrations. This was observed as narrow size distributions except with the highest L-leucine concentration (C_{re} = 0.41 g/m^3) that gave bimodal size distribution, see Fig. 4C. The bimodal size distribution indicated that several nucleation modes were occurring along the cooling zone. At high L-leucine concentrations, large amounts of L-leucine vapor underwent high momentary supersaturation in the cooling section, see Table 1. Thus, in addition to heterogeneous nucleation of L-leucine vapor on the surface of the core particles, pure L-leucine particles were able to form via homogeneous nucleation.

Fig. 5(A–C) shows the geometric number mean diameter (GNMD), number concentration (N), and G.S.D. of the salbutamol/L-leucine particles produced at different L-leucine concentrations and reactor temperatures. The size and concentration of the particles with C_{re} = 0.01–0.05 g/m^3 did not show any particular change with reactor temperature. The G.S.D. of these particles decreased at a certain temperature and then leveled off. Instead, the particle sizes and the G.S.D. of the two highest L-leucine concentrations increased in a discontinuous manner within the temperature range 145–160 °C. Obviously, the particles were formed in a different way than at T_H below 145 °C. This can be seen in Fig. 5C where the G.S.D. of particles with C_{re} = 0.10 and 0.41 g/m^3 increased within T_H = 140–145 and 145–155 °C, respectively. This was due to particle breakage as discussed earlier. Further increases in T_H resulted in increased particle size and decreased G.S.D. and a simultaneous decrease in the number of particles with C_{re} = 0.41 g/m^3 (Fig. 5A and B). The increasing sublimation of L-leucine at higher temperatures prevented the formation of an impermeable surface crust due to the partial vaporization of L-leucine. The narrowing of size distributions, i.e., the decrease in G.S.D. was a good indication for the sublimation of L-leucine in the heated section and subsequent heterogeneous nucleation of L-leucine vapor on core particle surfaces in the cooling section of the reactor. However, the partial vapor pressures of L-leucine in the heated zone of the reactor indicated that L-leucine was not completely in the vapor phase at the intermediate temperatures in Case II. At the temperatures where L-leucine partially sublimed the two coating layers of L-leucine on the salbutamol core particles were likely to form: an inner layer via surface diffusion and an outer layer by the physical vapor deposition of L-leucine.

3.3. Morphology of L-leucine coated particles

Fig. 6 shows SEM images of particles produced under varying experimental conditions. The sizes of the particles are in a good agreement with volume-based median diameters calculated by Hatch-Choate conversion equations (Hinds, 1999): the diameters ranged from 140 to 598 nm. Pure salbutamol sulphate particles, i.e., without L-leucine, were spherical. However, particle morphology changed notably with the addition of L-leucine. The particles produced at reactor temperatures at which particles were formed by the drying of droplets (Case I), were collapsed or wrinkled. This case applies to images A–C and F in Fig. 6. The morphology of these particles was related to the removal of water from the particle interior through the L-leucine film as discussed above. Also, fractured particles were observed as the concentration of L-leucine increased. As the saturation conditions shifted to favor sublimation, the saturation ratio was at the vicinity of unity, a fraction of L-leucine sublimed and nucleated in the later step on the core particle surfaces (Case II). This case applies to the image E in Fig. 6. During the course of sublimation, the amount of L-leucine decreased on the salbutamol particle surface. The shape of salbutamol/L-leucine particles changed close to the original spherical shape. When L-leucine was discharged from the surface, salbutamol in the fluidic state, i.e., at temperature above the glass transition temperature was able to resume the spherical shape. The glass transition temperature of salbutamol sulphate is 64 °C (Ward and Schultz, 1995). These particles consisted of two L-leucine coating layers, one layer by diffusion onto the droplet surface and the second layer by vapor deposition of L-leucine. When the saturation conditions for L-leucine favored

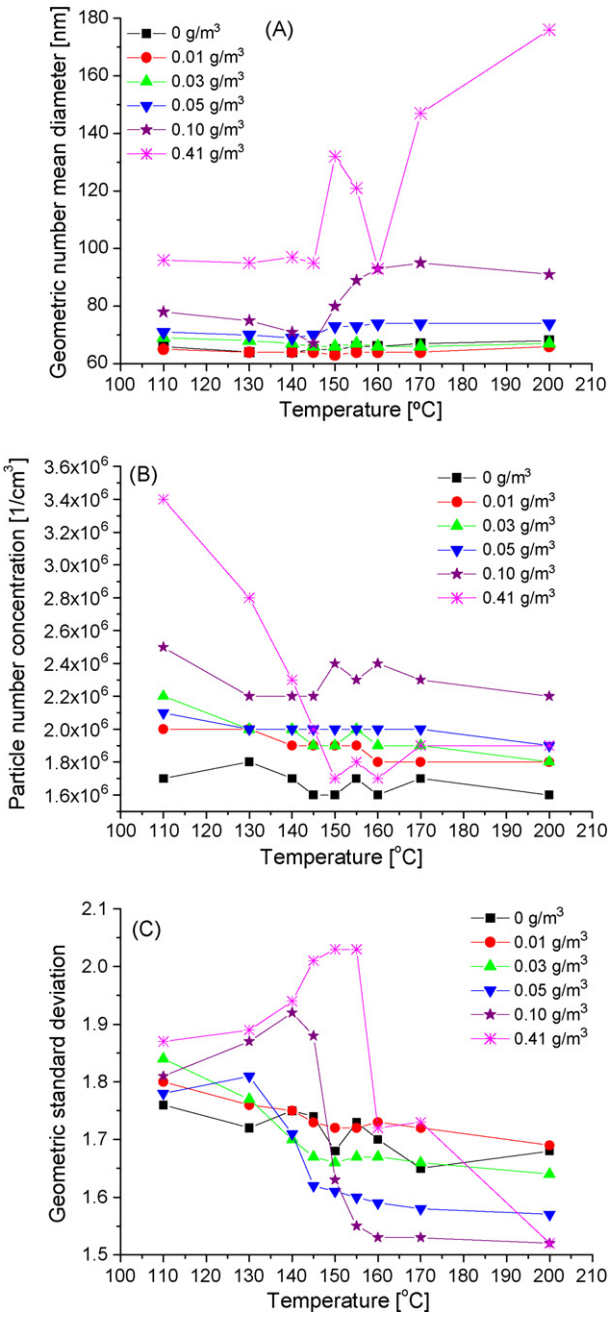

Fig. 5. Characteristics of the salbutamol/L-leucine particles produced under varying saturation conditions of L-leucine (C_{sal} = 0.10 g/m^3, C_{re} = 0–0.41 g/m^3): (A) geometric number mean diameter (GNMD), (B) particle number concentration (N) and (C) geometric standard deviation (G.S.D.).

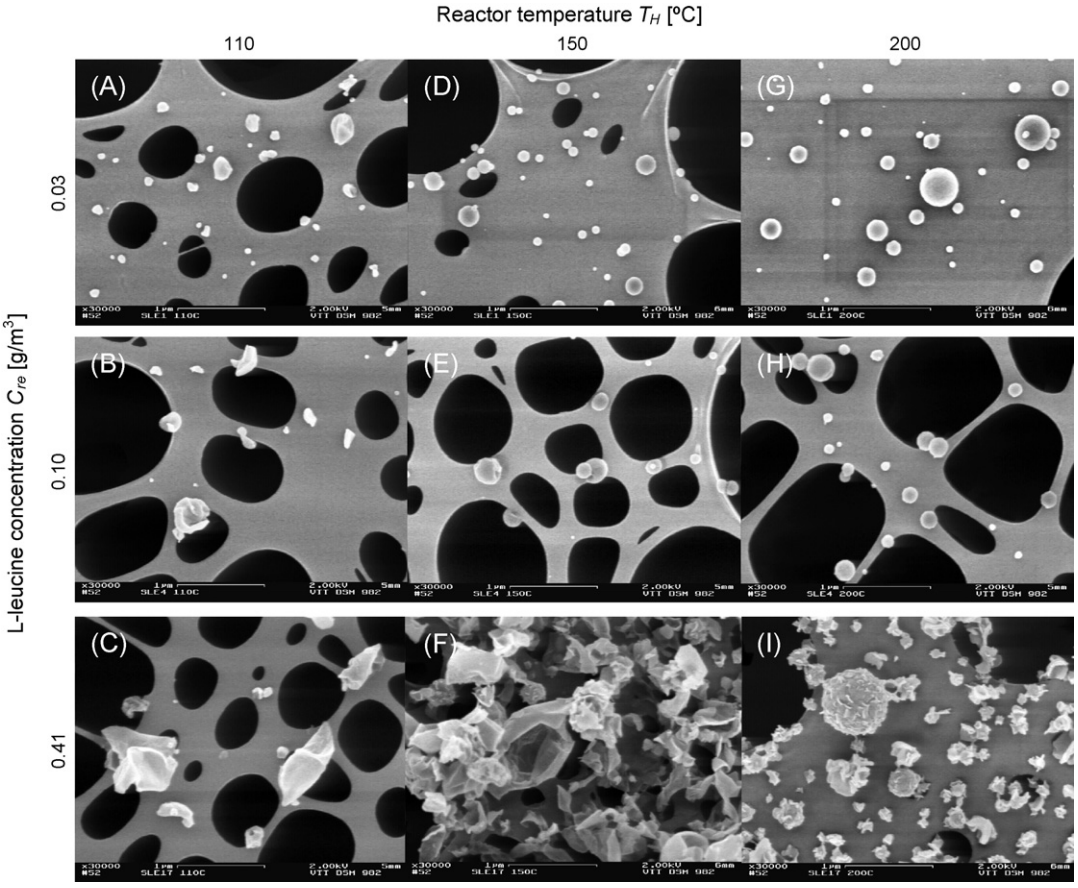

Fig. 6. SEM images of salbutamol/L-leucine particles produced at T_H of 110 °C (A–C) 150 °C (D–F) and 200 °C (G–I) under varying L-leucine concentration (C_{sal} = 0.10 g/m^3, C_{re} = 0.03–0.41 g/m^3).

a complete sublimation the cores of the particles were spherical coated with L-leucine crystals formed via vapor deposition (Case III). This applied to images D, and G–I in Fig. 6. At the highest L-leucine concentration (Fig. 6) the growth of L-leucine crystals on the particle surface was evident. Upon nucleation and deposition of vapor, L-leucine is known to form flaky crystals a few nanometers in size (Raula et al., 2007).

4. Conclusions

We have presented a method for the simultaneous synthesis and coating of gas-borne nanoparticles using physical vapor deposition of the amino acid L-leucine in an aerosol flow reactor. The nanoparticle cores with a geometric size of approximately 65 nm consisting of salbutamol sulphate were coated with L-leucine under various saturation conditions of L-leucine, i.e., the saturation ratio was below and above unity. Before coating, aqueous solute droplets were dried, followed by the sublimation of L-leucine from dry core particles. The nucleation and deposition of L-leucine vapor on the nanoparticle surfaces were carried out upon rapid cooling of L-leucine vapor leading to supersaturation of vapor. The formation of L-leucine coated nanoparticles was classified into three different mechanisms according to the partial vapor pressure of L-leucine in the heated zone, i.e., the saturation conditions. Depending on the conditions the L-leucine coating layer was formed either by molecular diffusion on droplet surfaces or by vapor deposition of L-leucine vapor on the core particle. When the saturation conditions were at the vicinity of unity, L-leucine vaporized only partially leading to the formation of two separate coating layers on the core particles. The pure salbutamol nanoparticles were spherical, however, the morphology of these particles changed to wrinkled (drying of droplets) or to spheres with leafy-looking L-leucine crystals on the surface. The developed method allowed the gas-phase coating of individual nanoparticles where the L-leucine coating could be tailored according to its solid–vapor state.

Acknowledgements

We thank Academy of Finland for financial support. The authors wish to thank Sini Anttalainen for help in the experiments.

References

Bodmeier, R., Chen, H., Tyle, P., Jarosz, P., 1991. Spontaneous formation of drug-containing acrylic nanoparticles. J. Microencaps 8, 161–170.
Budavari, S., O'Neil, M.J., Smith, A., Heckelman, P.E., 1989. The Merck Index, 11th ed. Merck & Co., Inc., Rahway, NJ, USA.
Brigger, I., Dubernet, C., Couvreur, P., 2002. Nanoparticles in cancer therapy and diagnosis. Adv. Drug. Deliv. Rev. 54, 631–651.
Chen, X., Young, T.J., Sarkari, M., Williams III, R.O., Johnston, K.P., 2002. Preparation of cyclosporine A nanoparticles by evaporative precipitation into aqueous solution. Int. J. Pharm. 242, 3–14.
Chew, N.Y.K., Shekunov, B.Y., Tong, H.H.Y., Chow, A.H.L., Savage, C., Wu, J., Chan, H.-K., 2005. Effect of amino acids on the dispersion of disodium cromglycate powders. J. Pharm. Sci. 94, 2289–2300.

Choy, K.L., 2003. Chemical vapour deposition coatings. Prog. Mater. Sci. 48, 57–170.
Cooney, D.J., Hickey, A.J., 2003. Preparation of disodium fluorescein powders in association with lauric and capric acids. J. Pharm. Sci. 92, 2341–2344.
Dick, K., Dhanasekaran, T., Zhang, Z., Meisel, D., 2002. Size-dependent melting of silica-encapsulated gold nanoparticles. J. Am. Chem. Soc. 124, 2312–2317.
Edwards, D.A., Hanes, J., Caponetti, G., Hrkach, J., Ben-Jebria, A., Eskew, M.L., Mintzes, J., Deaver, D., Lotan, N., Langer, R., 1997. Large porous particles for pulmonary drug delivery. Science 276, 1868–1871.
Gurav, A., Kodas, T., Pluym, T., Xiong, Y., 1993. Aerosol processing of materials. J. Aerosol Sci. 19, 411–452.
Hinds, W.C., 1999. Aerosol Technology: Properties, Behaviour and Measurement of Airborne Particles, 2nd ed. John Wiley & Sons, Inc., New York, USA.
Ichikawa, H., Fukumori, Y., 1999. Migroagglomeration of pulverized pharmaceutical powders using the Wurster process I. Preparation of highly drug-incorporated, subsieve-sized core particles for subsequent microencapsulation by film coating. Int. J. Pharm. 180, 195–210.
Incropera, F.P., DeWitt, D.P., 2002. Fundamentals of Heat and Mass Transfer, 5th edn. John Wiley & Sons, Inc., New York, USA.
Jiang, Q., Shi, H.X., Zhao, M., 1999. Melting thermodynamics of organic nanocrystals. J. Chem. Phys. 111, 2176–2180.
Jiang, Q., Zhang, Z., Li, J.C., 2000. Melting thermodynamics of nanocrystals embedded in a matrix. Acta Mater. 48, 4791–4795.
Lai, S.L., Guo, J.Y., Petrova, V., Ramanath, G., Allen, L.H., 1996. Size-dependent melting properties of small tin particles: nanocalorimetric measurements. Phys. Rev. Lett. 77, 99–102.
Lechuga-Ballesteros, D., Kuo, M.-C., 2001. Dry powder compositions having improved dispersivity. WO 01/32144.
Lucas, P., Anderson, K., Potter, U.J., Staniforth, J.N., 1999. Enhancement of small particle size dry powder aerosol formulations using an ultra low density additive. Pharm. Res. 16, 1643–1647.
Lähde, A., Raula, J., Kauppinen, E.I., Watanabe, W., Ahonen, P.P., Brown, D.P., 2006. Aerosol synthesis of inhalation particles via a droplet-to-particle method. Part. Sci. Technol. 24, 71–84.
Mattox, D.M., 1998. Handbook of Physical Vapour Deposition (PVD) Processing. William Andrew Publishing/Noyes, Park Ridge.
Murakami, H., Kobayashi, M., Takeuchi, H., Kawashima, Y., 1999. Preparation of poly(DL-lactide-co-glycolide) nanoparticles modified spontaneous emulsification solvent diffusion method. Int. J. Pharm. 187, 143–152.
Obersdörster, G., Obserdörster, E., Obserdörster, J., 2005. Nanotoxicology: an emerging discipline evolving from studies of ultrafine particles. Environ. Health Persp. 113, 823–839.
Peltonen, L., Koistinen, P., Karjalainen, M., Häkkinen, A., Hirvonen, J., 2002. The effect of cosolvents on the formulation of nanoparticles from low-molecular-weight poly(l)lactide. AAPS Pharm. Sci. Tech. 3, E32.
Pfeffer, R., Dave, R.N., Wei, D., Ramlakhan, M., 2001. Synthesis of engineered particulates with tailored properties using dry particle coating. Powder Tech. 117, 40–67.
Pillai, R.S., Yeates, D.B., Miller, I.F., Hickey, A.J., 1994. Controlled release from condensation coated respirable aerosol particles. J. Aerosol Sci. 25, 461–477.
Ramlakhan, M., Wu, C.Y., Watano, S., Dave, R.N., Pfeffer, R., 2000. Dry particle coating using magnetically assisted impaction coating: modification of surface properties and optimization of system and operating parameters. Powder Tech. 112, 137–148.
Raula, J., Lähde, A., Kauppinen, E.I., 2008. A novel gas phase method for the combined synthesis and coating of pharmaceutical particles. Pharm. Res. 25, 242–245.
Raula, J., Kuivalainen, A., Lähde, A., Antopolsky, M., Kansikas, J., Kauppinen, E.I., 2007. Synthesis of L-leucine nanoparticles via physical vapor deposition at varying saturation conditions. J. Aerosol Sci. 38, 1172–1184.
Ravi Kumar, M.N.V., 2000. Nano and microparticles as controlled drug delivery devices. J. Pharm. Sci. 3, 234–258.
Ré, M.I., 1998. Microencapsulation by spray drying. Drying Tech. 16, 1195–1236.
Schmidt, C., Bodmeier, R., 1999. Incorporation of polymeric nanoparticles into solid dosage forms. J. Controlled Release 57, 115–125.
Seinfeld, J.H., Pandis, S.N., 2006. Atmospheric Chemistry and Physics: From Air Pollution to Climate Change, 2nd edn. John Wiley & Sons, Inc., New Jersey, USA.
Svec, H.J., Clyde, D.D., 1965. Vapor pressures of some amino acids. J. Chem. Eng. Data 10, 151–152.
Ward, G.H., Schultz, R.K., 1995. Process-induced crystallinity changes in albuterol sulfate and its effect of powder physical stability. Pharm. Res. 12, 773–779.
Weissbuch, I., Frolow, F., Addadi, L., Lahav, M., Leiserowitz, L., 1990. Oriented crystallization as a tool for detecting ordered aggregates of water-soluble hydrophobic α-amino acids at the air-solution interface. J. Am. Chem. Soc. 112, 7718–7724.
Yang, J., Sliva, A., Banerjee, A., Dave, R.N., Pfeffer, R., 2005. Dry particle coating for improving the flowability of cohesive powders. Powder Tech. 158, 21–33.
Zhang, L., Ranade, M.B., Gentry, J.W., 2004. Formation of organic coating on ultrafine silver particles using a gas-phase process. J. Aerosol Sci. 35, 457–471.
Zhao, M., Jiang, Q., 2004. Melting and surface melting of low-dimensional in crystals. Solid State Commun. 130, 37–39.